

## Parametric identification of a cable-stayed bridge using least square estimation with substructure approach

Hongwei Huang<sup>\*1,2</sup>, Yaohua Yang<sup>2a</sup> and Limin Sun<sup>1,2b</sup>

<sup>1</sup>State Key Laboratory for Disaster Reduction in Civil Engineering, Tongji University, Shanghai, China

<sup>2</sup>Department of Bridge Engineering, Tongji University, Shanghai, China

(Received November 19, 2014, Revised January 14, 2015, Accepted January 16, 2014)

**Abstract.** Parametric identification of structures is one of the important aspects of structural health monitoring. Most of the techniques available in the literature have been proved to be effective for structures with small degree of freedoms. However, the problem becomes challenging when the structure system is large, such as bridge structures. Therefore, it is highly desirable to develop parametric identification methods that are applicable to complex structures. In this paper, the LSE based techniques will be combined with the substructure approach for identifying the parameters of a cable-stayed bridge with large degree of freedoms. Numerical analysis has been carried out for substructures extracted from the 2-dimensional (2D) finite element model of a cable-stayed bridge. Only vertical white noise excitations are applied to the structure, and two different cases are considered where the structural damping is not included or included. Simulation results demonstrate that the proposed approach is capable of identifying the structural parameters with high accuracy without measurement noises.

**Keywords:** parametric identification; cable-stayed bridge; least square estimation; substructure approach

### 1. Introduction

Parametric identification based on vibration characteristics provides useful information for both real-time online monitoring and overall offline evaluation of structures. The modal parameters (such as damping and frequency) of structure vibrations are dependent variables that relate to physical parameters (such as mass and stiffness). Therefore, accurate identification of structure parameters is the premise of a reasonable structure health monitoring system. Various analysis methodologies for parametric identifications have been derived (e.g., Bernal and Beck 2004, Lin *et al.* 2005, Zhou and Yan 2006, Lei *et al.* 2012). However, the problem becomes challenging when the structure system is large and complex, for example, bridge structures where the number of degree of freedom (DOF) is huge, because most of the identification methods available in the literature have better accuracy and adaptability for relatively small DOF structural systems (e.g., Caravani *et al.* 1977, Yang and Lin 2004, 2005, Yang *et al.* 2007).

Therefore, in order to ensure accurate identification of structural parameters of bridges,

---

\*Corresponding author, Associate Professor, E-mail: hongweih@tongji.edu.cn

<sup>a</sup> Graduate Student

<sup>b</sup> Professor

different approaches have been proposed. For example, the integration of GPS technology and accelerometers has been shown to be effective in characterizing the dynamic behavior of bridge structures (Yi *et al.* 2010, 2013a), the multi-stage structural damage diagnosis method is proved to be computational efficient in assessing damages in large structures (Yi *et al.* 2013b), and substructure approach can be used to decompose the complex structure having multiple DOFs into smaller parts such that the number of unknowns is limited within a certain range (Koh *et al.* 1991, 2003, Law and Yong 2011, Wen *et al.* 2012, Lei *et al.* 2013). In particular, Koh *et al.* (1991, 2003) conducted systematic studies on the parametric identification of structures with different scales and conditions using genetic algorithm and found that the accuracy of substructure identification approach is higher than full structure identification method and requires much less computational time.

In this paper, the substructure approach proposed in Koh *et al.* (2003) will be combined with the least square estimation (LSE) method given in Yang and Lin (2004, 2005) for identifying the parameters of a cable-stayed bridge with large DOFs. Numerical analysis has been carried out for substructures extracted from the 2-dimensional (2D) finite element model of a cable-stayed bridge. Only vertical white noise excitations are applied to the structure, and two different cases are considered where the structural damping is not included or included. Simulation results demonstrate that the proposed approach is capable of identifying the structural parameters with high accuracy without measurement noises.

## 2. Fundamental theory

### 2.1 Substructure approach

The equation of motion (EOM) for a complete structural system can be written as

$$\mathbf{M}\ddot{\mathbf{x}}(t) + \mathbf{C}\dot{\mathbf{x}}(t) + \mathbf{K}\mathbf{x}(t) = \mathbf{F}(t) \quad (1)$$

where  $\mathbf{M}$ ,  $\mathbf{C}$ ,  $\mathbf{K}$  are the mass, damping and stiffness matrices, respectively,  $\mathbf{x}(t)$  is the displacement vector and  $\mathbf{F}(t)$  is the excitation force vector.

Consider a complex structure and suppose we are interested in monitoring some critical areas where damages may occur. A substructure containing that critical area can be extracted from the full structure, the corresponding EOM may be written by partitioning the original matrices and vectors as follows

$$\begin{aligned} & \begin{pmatrix} \mathbf{M}_{ff} & \mathbf{M}_{fr} & \mathbf{0} \\ \mathbf{M}_{rf} & \mathbf{M}_{rr} & \mathbf{M}_{rg} \\ \mathbf{0} & \mathbf{M}_{gr} & \mathbf{M}_{gg} \end{pmatrix} \begin{bmatrix} \ddot{\mathbf{x}}_f(t) \\ \ddot{\mathbf{x}}_r(t) \\ \ddot{\mathbf{x}}_g(t) \end{bmatrix} + \begin{pmatrix} \mathbf{C}_{ff} & \mathbf{C}_{fr} & \mathbf{0} \\ \mathbf{C}_{rf} & \mathbf{C}_{rr} & \mathbf{C}_{rg} \\ \mathbf{0} & \mathbf{C}_{gr} & \mathbf{C}_{gg} \end{pmatrix} \begin{bmatrix} \dot{\mathbf{x}}_f(t) \\ \dot{\mathbf{x}}_r(t) \\ \dot{\mathbf{x}}_g(t) \end{bmatrix} \\ & + \begin{pmatrix} \mathbf{K}_{ff} & \mathbf{K}_{fr} & \mathbf{0} \\ \mathbf{K}_{rf} & \mathbf{K}_{rr} & \mathbf{K}_{rg} \\ \mathbf{0} & \mathbf{K}_{gr} & \mathbf{K}_{gg} \end{pmatrix} \begin{bmatrix} \mathbf{x}_f(t) \\ \mathbf{x}_r(t) \\ \mathbf{x}_g(t) \end{bmatrix} = \begin{bmatrix} \mathbf{F}_f(t) \\ \mathbf{F}_r(t) \\ \mathbf{F}_g(t) \end{bmatrix} \end{aligned} \quad (2)$$

where subscripts ‘ $f$ ’ and ‘ $g$ ’ denote the interface DOFs at the two ends of the substructure and subscript ‘ $r$ ’ denotes the internal DOFs (Koh *et al.* 1991). Since we are interested in identifying the parameters within the substructure, only the second equation of Eq. (2) will be used, i.e.

$$\begin{aligned} \mathbf{M}_{rf} \ddot{\mathbf{x}}_f(t) + \mathbf{M}_{rr} \ddot{\mathbf{x}}_r(t) + \mathbf{M}_{rg} \ddot{\mathbf{x}}_g(t) + \mathbf{C}_{rf} \dot{\mathbf{x}}_f(t) + \mathbf{C}_{rr} \dot{\mathbf{x}}_r(t) + \mathbf{C}_{rg} \dot{\mathbf{x}}_g(t) \\ + \mathbf{K}_{rf} \mathbf{x}_f(t) + \mathbf{K}_{rr} \mathbf{x}_r(t) + \mathbf{K}_{rg} \mathbf{x}_g(t) = \mathbf{F}_r(t) \end{aligned} \quad (3)$$

For parametric identification, we can rearrange all the interface DOFs to the right hand side of the above equation and treat them as inputs (excitations) to the substructure. Then, Eq. (3) can be expressed as

$$\mathbf{M}_{rr} \ddot{\mathbf{x}}_r(t) + \mathbf{C}_{rr} \dot{\mathbf{x}}_r(t) + \mathbf{K}_{rr} \mathbf{x}_r(t) = \mathbf{F}_{eq}(t) \quad (4)$$

$$\begin{aligned} \mathbf{F}_{eq}(t) = \mathbf{F}_r(t) - \mathbf{M}_{rf} \ddot{\mathbf{x}}_f(t) + \mathbf{M}_{rg} \ddot{\mathbf{x}}_g(t) \\ + \mathbf{C}_{rf} \dot{\mathbf{x}}_f(t) + \mathbf{C}_{rg} \dot{\mathbf{x}}_g(t) + \mathbf{K}_{rg} \mathbf{x}_g(t) + \mathbf{K}_{rf} \mathbf{x}_f(t) \end{aligned} \quad (5)$$

where  $\ddot{\mathbf{x}}_r(t)$ ,  $\dot{\mathbf{x}}_r(t)$ ,  $\mathbf{x}_r(t)$  are the output (measured) acceleration, velocity and displacement responses, respectively (Koh *et al.* 1991).

## 2.2 Least square estimation (LSE)

Supposed  $\boldsymbol{\theta}(t)$  is an  $n$ -parametric vector consisting of  $n$  unknown parameters, including damping, stiffness, and nonlinear parameters, i.e.,

$$\boldsymbol{\theta}(t) = [\theta_1(t) \quad \theta_2(t) \quad \cdots \quad \theta_n(t)]^T \quad (6)$$

The observation equation associated with the EOM of Eq. (1) can be written as

$$\boldsymbol{\varphi}[\ddot{\mathbf{x}}(t), \dot{\mathbf{x}}(t), \mathbf{x}(t); t] \boldsymbol{\theta}(t) + \boldsymbol{\varepsilon}(t) = \mathbf{y}(t) \quad (7)$$

where  $\ddot{\mathbf{x}}(t)$ ,  $\dot{\mathbf{x}}(t)$ ,  $\mathbf{x}(t)$  are  $m$ -measured acceleration, velocity, displacement response vectors;  $\mathbf{y}(t)$  is  $m$ -measured output vector;  $\boldsymbol{\varepsilon}(t)$  is  $m$ -model noise vector contributed by the measurement noise and possible model errors; and  $\boldsymbol{\varphi}[\ ]$  is  $(m \times n)$  observation matrix.

At each time instant  $t = t_{k+1} = (k+1)\Delta t$ , Eq. (7) can be discretized as

$$\boldsymbol{\varphi}_{k+1} \boldsymbol{\theta}_{k+1} + \boldsymbol{\varepsilon}_{k+1} = \mathbf{y}_{k+1} \quad (8)$$

Combining all equations in Eq. (8) for  $k+1$  time instants, and assuming that  $\boldsymbol{\theta}_{k+1}$  is a constant vector, one obtains

$$\boldsymbol{\phi}_{k+1} \boldsymbol{\theta}_{k+1} + \mathbf{E}_{k+1} = \mathbf{Y}_{k+1} \quad (9)$$

Where

$$\boldsymbol{\phi}_{k+1} = \begin{pmatrix} \boldsymbol{\varphi}_1 \\ \boldsymbol{\varphi}_2 \\ \vdots \\ \boldsymbol{\varphi}_{k+1} \end{pmatrix}, \quad \mathbf{E}_{k+1} = \begin{pmatrix} \boldsymbol{\varepsilon}_1 \\ \boldsymbol{\varepsilon}_2 \\ \vdots \\ \boldsymbol{\varepsilon}_{k+1} \end{pmatrix}, \quad \mathbf{Y}_{k+1} = \begin{pmatrix} \mathbf{y}_1 \\ \mathbf{y}_2 \\ \vdots \\ \mathbf{y}_{k+1} \end{pmatrix}; \quad (10)$$

Let  $\hat{\boldsymbol{\theta}}_{k+1}$  be the estimate of  $\boldsymbol{\theta}_{k+1}$  at  $t_{k+1} = (k+1)\Delta t$ , the recursive solution for  $\hat{\boldsymbol{\theta}}_{k+1}$  can be obtained as

$$\hat{\boldsymbol{\theta}}_{k+1} = \hat{\boldsymbol{\theta}}_k + \mathbf{G}_{k+1} (\mathbf{y}_{k+1} - \boldsymbol{\varphi}_{k+1} \hat{\boldsymbol{\theta}}_k) \quad (11)$$

in which

$$\mathbf{G}_{k+1} = \mathbf{P}_k \boldsymbol{\varphi}_{k+1}^T (\mathbf{I} + \boldsymbol{\varphi}_{k+1} \mathbf{P}_k \boldsymbol{\varphi}_{k+1}^T)^{-1} \quad (12)$$

$$\mathbf{P}_{k+1} = (\mathbf{I} - \mathbf{G}_{k+1} \boldsymbol{\varphi}_{k+1}) \mathbf{P}_k \quad (13)$$

where  $\mathbf{G}_{k+1}$  is the LSE gain matrix, Eqs. (10)-(12) are the recursive solution of classic LSE method (Yang and Lin 2005).

### 2.3 Combination of substructure and LSE methods

In order to identify unknown structural parameters using both methods in the numerical study, Rayleigh damping is assumed for the substructure as

$$\mathbf{C}_{sb} = \alpha \mathbf{M}_{sb} + \beta (\mathbf{K}_{sb} - \mathbf{K}_{Gsb}) \quad (14)$$

where subscripts 'sb' denotes substructure;  $\alpha$  and  $\beta$  are the mass and stiffness damping coefficient respectively;  $\mathbf{K}_{sb}$  and  $\mathbf{K}_{Gsb}$  are the substructure stiffness and geometric stiffness matrices respectively;  $\mathbf{M}_{sb}$  is the substructure mass matrix. For time instant  $t_k$ , the EOM can be presented as

$$(\mathbf{K}_{sb} - \mathbf{K}_{Gsb}) \mathbf{x}(t_k) + [\alpha \mathbf{M}_{sb} + \beta (\mathbf{K}_{sb} - \mathbf{K}_{Gsb})] \dot{\mathbf{x}}(t_k) + \mathbf{M}_{sb} \ddot{\mathbf{x}}(t_k) = \mathbf{F}_{eq}(t_k) \quad (15)$$

In the finite element modeling, the substructure stiffness matrix  $\mathbf{K}_{sb}$  is assembled from element stiffness matrix  $\mathbf{K}_i^e$ , in which  $i$  denotes the element number, and Eq. (15) can be transformed to

$$\begin{aligned} & \sum_{i=1}^n \mathbf{K}_i^e \mathbf{x}(t_k) + \sum_{i=1}^n \beta \mathbf{K}_i^e \dot{\mathbf{x}}(t_k) - \beta \mathbf{K}_{Gsb} \dot{\mathbf{x}}(t_k) + \alpha \mathbf{M}_{sb} \ddot{\mathbf{x}}(t_k) \\ & = \mathbf{F}_{eq}(t_k) + \mathbf{K}_{Gsb} \mathbf{x}(t_k) - \mathbf{M}_{sb} \ddot{\mathbf{x}}(t_k) \end{aligned} \quad (16)$$

where  $n$  denotes total number of elements. Since  $\mathbf{K}_{Gsb}$  and  $\mathbf{M}_{sb}$  are regarded as known value and  $\mathbf{F}_{eq}(t_k)$ ,  $\ddot{\mathbf{x}}(t_k)$  and  $\mathbf{x}(t_k)$  are measured vectors, the right hand side of the above equation corresponds to  $\mathbf{y}(t)$  while the left hand side corresponds to  $\boldsymbol{\varphi}\boldsymbol{\theta}(t)$  in Eq. (7). Let the stiffness

$(EI)_i$  of each element be the unknown parameter to be identified, the stiffness matrix of beam element without axial deformation can be written as

$$\mathbf{K}_i^e = k_i \mathbf{S}_i^e = (EI)_i \times \frac{2}{l_i^3} \begin{pmatrix} 6 & 3l_i & -6 & 3l_i \\ 3l_i & 2l_i^2 & -3l_i & l_i^2 \\ -6 & -3l_i & 6 & -3l_i \\ 3l_i & l_i^2 & -3l_i & 2l_i^2 \end{pmatrix} \quad (17)$$

where  $k_i = (EI)_i$ . After expanding  $\mathbf{K}_i^e$  to the global coordinate system as  $\mathbf{K}_{sb}$ , one has

$$\mathbf{K}_i^e \mathbf{x}(t_k) = (EI)_i [\mathbf{S}_i^e \mathbf{x}(t_k)] = k_i [\mathbf{S}_i^e \mathbf{x}(t_k)] \quad (18)$$

in which  $[\mathbf{S}_i^e \mathbf{x}(t_k)]$  is a vector whose dimension is the same as  $\mathbf{F}_{eq}(t_k)$ . Similar expansion applies to  $(EA)_i, \alpha$ , and  $\beta$ . Then, the left hand side of Eq. (16) can be transformed to

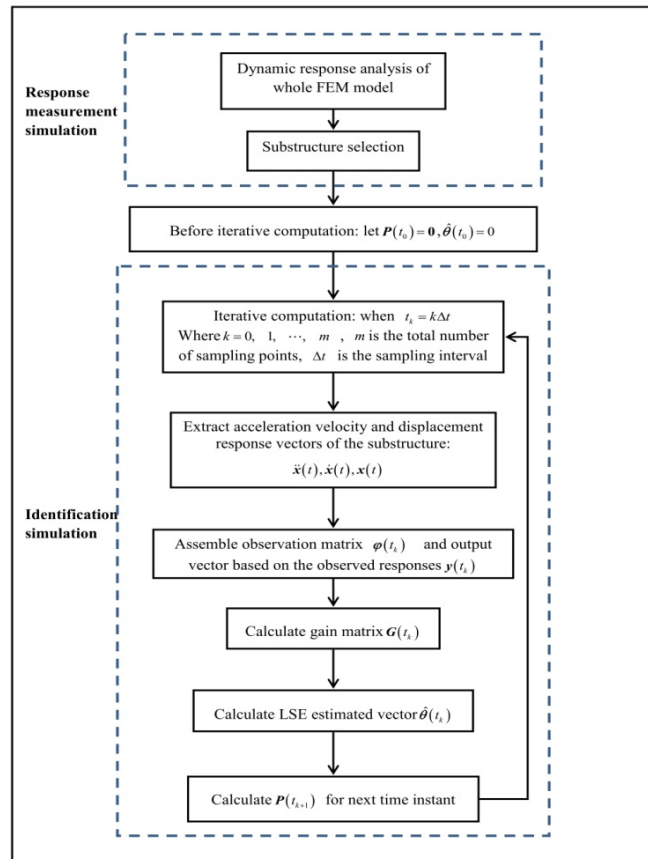


Fig. 1 Program flow chart

$$\sum_{i=1}^n \mathbf{K}_i^e \mathbf{x}(t_k) + \sum_{i=1}^n \beta \mathbf{K}_i^e \dot{\mathbf{x}}(t_k) - \beta \mathbf{K}_{Gsb} \dot{\mathbf{x}}(t_k) + \alpha \mathbf{M}_{sb} \ddot{\mathbf{x}}(t_k) = \boldsymbol{\varphi}(t_k) \boldsymbol{\theta}(t_k) \quad (19)$$

$$\boldsymbol{\varphi}(t_k) = \left( \mathbf{S}_1^e \mathbf{x} \quad \mathbf{S}_2^e \mathbf{x} \quad \cdots \quad \mathbf{S}_n^e \mathbf{x}, \quad \mathbf{S}_1^e \dot{\mathbf{x}} \quad \mathbf{S}_2^e \dot{\mathbf{x}} \quad \cdots \quad \mathbf{S}_n^e \dot{\mathbf{x}}, \quad -\mathbf{K}_{Gsb} \dot{\mathbf{x}}, \quad \mathbf{M}_{sb} \ddot{\mathbf{x}} \right) \quad (20)$$

$$\boldsymbol{\theta}(t_k) = \left( k_1 \quad k_2 \quad \cdots \quad k_n, \quad \beta k_1 \quad \beta k_2 \quad \cdots \quad \beta k_n, \quad \beta, \quad \alpha \right)^T \quad (21)$$

Hence, the observation equation and the corresponding matrices and vectors for substructure identification can be summarized as follows

$$\boldsymbol{\varphi}(t_k) \boldsymbol{\theta}(t_k) = \mathbf{y}(t_k) \quad (22)$$

$$\boldsymbol{\varphi}(t_k) = \left( \mathbf{S}_1^e \mathbf{x} \quad \mathbf{S}_2^e \mathbf{x} \quad \cdots \quad \mathbf{S}_n^e \mathbf{x}, \quad \mathbf{S}_1^e \dot{\mathbf{x}} \quad \mathbf{S}_2^e \dot{\mathbf{x}} \quad \cdots \quad \mathbf{S}_n^e \dot{\mathbf{x}}, \quad -\mathbf{K}_{Gsb} \dot{\mathbf{x}}, \quad \mathbf{M}_{sb} \ddot{\mathbf{x}} \right) \quad (23)$$

$$\boldsymbol{\theta}(t_k) = \left( k_1 \quad k_2 \quad \cdots \quad k_n, \quad \beta k_1 \quad \beta k_2 \quad \cdots \quad \beta k_n, \quad \beta, \quad \alpha \right)^T \quad (24)$$

$$\mathbf{y}(t_k) = \mathbf{F}_{eq}(t_k) + \mathbf{K}_{Gsb} \mathbf{x}(t_k) - \mathbf{M}_{sb} \ddot{\mathbf{x}}(t_k) \quad (25)$$

Fig. 1 shows the flow chart for carrying out the parametric identification using LSE method combined with substructure approach.

### 3. Numerical model of a cable-stayed bridge

In this paper, the Kezhushan Bridge which is one of the main navigation channels of Donghai bridge located in Shanghai, China will be studied using numerical simulation. The bridge is 710 meters long with a main span of 332 meters and two side spans of 139 meters each and the full wide is 35 meters. It is a steel-concrete composite beam structure with two pylons and double cable planes. Each of the pylons is a reinforced concrete structure of 105 meters high. Cables are shaped into sectors and disposed symmetrically and each cable plane has 64 (2×32) cables. The general layout of the bridge is shown in Fig. 2.

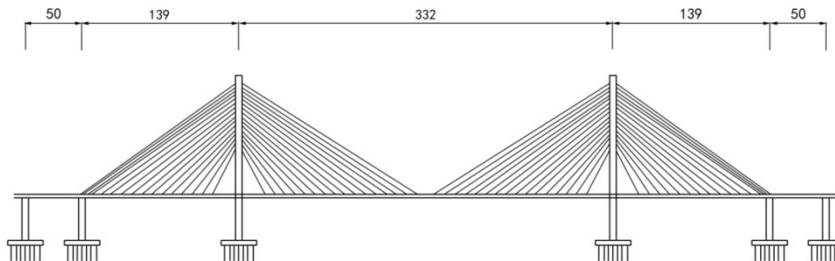


Fig. 2 The general layout of Kezhushan Bridge

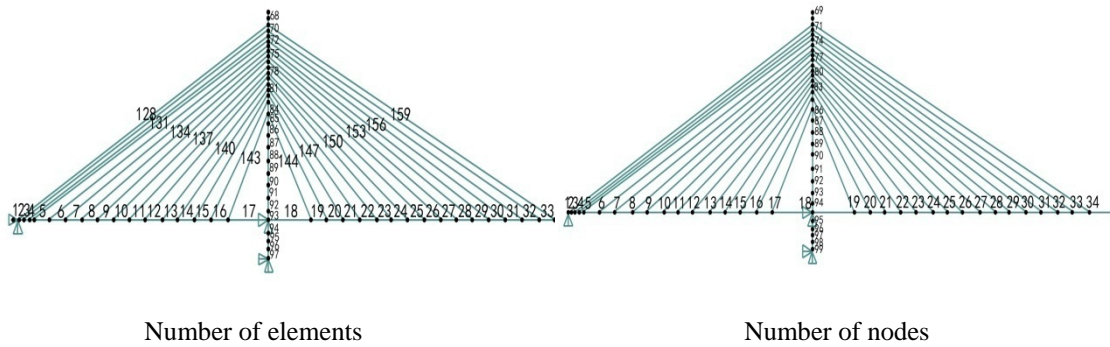


Fig. 3 Numbering of elements and nodes of half model

### 3.1 Simplified model

As this paper focuses on the vibrations of bridge under vertical excitations such as traffic loads, for the simplification of analysis, a 2-dimensionanl (2D) model is established in the numerical study, consisting of a beam, two towers and 64 cables. The cross section of a tower or a cable is two times of the original ones, since parallel cables or towers are combined into one. The axial deformation of beam and tower elements is ignored.

The finite element model of the bridge is set up with numbering of nodes and elements shown in Fig. 3. The beam element is chosen between adjacent cable nodes and numbered from left to right as 1-67 where the nodes are numbered as 1-68. On the upper tower, the elements are selected between adjacent cable nodes, while on the middle and lower tower, it is divided into 14 elements equally. Therefore, the entire tower has 30 elements and 31 nodes numbered as 68-97 and 69-99 respectively for the left tower, and as 98-127 and 100-130 respectively for the right tower. Each cable is taken as one element numbered from left to right as 128-191.

Since only vertical excitations are considered, the beam node has just vertical DOF while the tower node has horizontal DOF, and all the nodes at the boundaries are constrained.

In summary, the entire model has 191 elements, 130 nodes and 252 DOFs.

### 3.2 Element matrices

#### Beam and tower element stiffness matrix

The geometric stiffness should be considered for element stiffness matrix if considering the axial forces, one has

$$\bar{\mathbf{K}}^e = \mathbf{K}^e - \mathbf{K}_G^e \tag{26}$$

in which

$$\mathbf{K}^e = \frac{2EI}{l^3} \begin{pmatrix} 6 & 3l & -6 & 3l \\ 3l & 2l^2 & -3l & l^2 \\ -6 & -3l & 6 & -3l \\ 3l & l^2 & -3l & 2l^2 \end{pmatrix} \quad (27)$$

$$\mathbf{K}_G^e = \frac{N}{30l} \begin{pmatrix} 36 & 3l & -36 & 3l \\ 3l & 4l^2 & -3l & -l^2 \\ -36 & -3l & 36 & -3l \\ 3l & -l^2 & -3l & 4l^2 \end{pmatrix} \quad (28)$$

where  $E$ ,  $I$ ,  $N$  and  $l$  are the modulus of elasticity, moment of inertia, axial force of length of the element, respectively.

#### Beam and tower element mass matrix

Suppose mass is distributed evenly along the length of element, a consistent element mass matrix can be written as follows

$$\mathbf{M}^e = \frac{\bar{m}l}{420} \begin{pmatrix} 156 & 22l & 54 & -13l \\ 22l & 4l^2 & 13l & -3l^2 \\ 54 & 13l & 156 & -22l \\ -13l & -3l^2 & -22l & 4l^2 \end{pmatrix} \quad (29)$$

where  $\bar{m}$  is the linear density of element.

#### Cable element stiffness matrix

A cable element only has two DOFs, a vertical DOF at the beam side and a horizontal DOF at the tower side, and its stiffness matrix can be written as follows

$$\mathbf{K}^e = \frac{E_{eg}A}{l} \begin{pmatrix} \sin^2 a & -\sin a \cos a \\ -\sin a \cos a & \cos^2 a \end{pmatrix} \quad (30)$$

where  $E_{eg}$  is the modulus of elasticity modified by Ernst equation given in Eq. (31),  $A$  is the cross sectional area, and  $a$  is the horizontal angle of the cable.

$$E_{eg} = \frac{E}{1 + \frac{\gamma^2 l_h^2 E}{12\sigma^3}} \quad (31)$$

where  $\sigma$  is the initial tension stress,  $\gamma$  is the bulk density, and  $l_h$  is the horizontal length of the cable, respectively.

Table 1\_Frequencies of the first six modes of the bridge

| mode | Simplified model | ANSYS 3D model | error |
|------|------------------|----------------|-------|
| 1    | 0.4018 Hz        | 0.3979 Hz      | 0.98% |
| 2    | 0.5403 Hz        | 0.5079 Hz      | 6.38% |
| 3    | 0.7985 Hz        | 0.8124 Hz      | 1.71% |
| 4    | 0.9832 Hz        | 0.9215 Hz      | 6.70% |
| 5    | 1.1104 Hz        | 1.0320 Hz      | 7.60% |
| 6    | 1.3027 Hz        | 1.2253 Hz      | 6.32% |

#### Cable element mass matrix

The mass matrix of cable element can be obtained based on linear interpolation as follows

$$\mathbf{M}^e = \begin{pmatrix} \frac{1}{3} \bar{m} l \sin^2 a & \frac{1}{6} \bar{m} l \sin a \cos a \\ \frac{1}{6} \bar{m} l \sin a \cos a & \frac{1}{3} \bar{m} l \cos^2 a \end{pmatrix} \quad (32)$$

After establishing the mass and stiffness matrices, the frequencies of the first six modes of the simplified 2D bridge model can be computed. The results are compared with the frequencies obtained from the 3-dimensional (3D) model in Dong (2010), as summarized in Table 1. It shows that the 2D model can be used to represent the dynamic characteristics of the bridge with reasonable accuracy.

## 4. Identification of structural parameters

Because of the symmetry of the cable-stayed bridge, only the parameters of half of the model need to be identified and the structure is divided into three substructures. A vertical white noise excitation is applied at each beam node as shown in Fig. 4, with loading period of 10 seconds, and the corresponding responses are measured with sampling frequency of 1000 Hz.

The parameters to be identified are the stiffness of all elements, namely  $EI$  for beam and tower elements and  $EA$  for cable elements.

Two different cases are studied in the numerical simulation, i.e., the structure with no damping and with Rayleigh damping.

### 4.1 Structure without damping

#### Substructure 1

The beam of the left span of the bridge model and the cables attached to it are considered as substructure 1 as shown in Fig. 5.

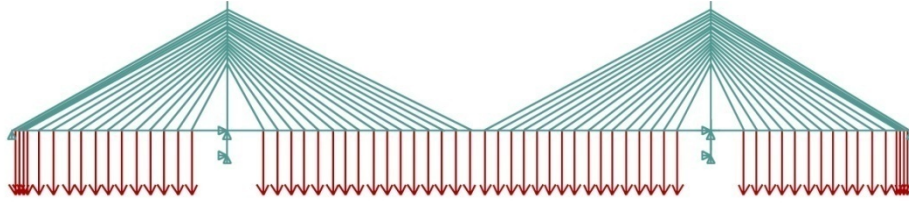


Fig. 4 Loading pattern of the bridge model

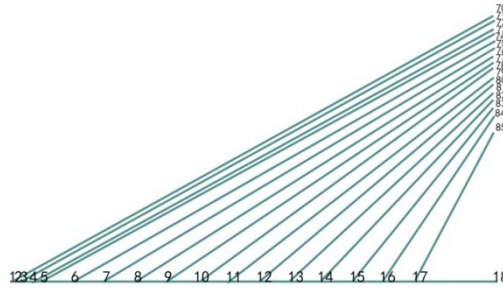


Fig. 5 Substructure 1

Substructure 1 contains NO.1-17 beam elements and NO.128-143 cable elements. The responses at the beam nodes and the cable nodes on the tower are considered as interface DOFs. There are 33 stiffness parameters to be identified for this substructure and the corresponding displacement vectors, parametric vectors, measurement vectors and observation matrices used in the LSE method are as follows

$$\mathbf{x} = (x_1 \ x_2 \ \cdots \ x_{34} \ , \ x_{135} \ x_{136} \ \cdots \ x_{165})^T \tag{33}$$

$$\boldsymbol{\theta} = (\theta_1 \ \theta_2 \ \cdots \ \theta_{17}, \ \theta_{128} \ \theta_{129} \ \cdots \ \theta_{143})^T \tag{34}$$

$$\mathbf{y} = (y_1 \ y_2 \ \cdots \ y_{33})^T \tag{35}$$

$$\boldsymbol{\varphi} = (S_1^e \mathbf{x} \ S_2^e \mathbf{x} \ \cdots \ S_{17}^e \mathbf{x}, \ S_{128}^e \mathbf{x} \ S_{129}^e \mathbf{x} \ \cdots \ S_{143}^e \mathbf{x}) \tag{36}$$

The results of identified structural parameters are presented in Table 2, where NO.1-17 lists the stiffness  $EI$  ( $10^{11} N \cdot m^2$ ) of beam elements and NO.18-33 gives the stiffness  $EA$  ( $10^9 N$ ) of cable elements.

Table 2 Identification parameters of substructure 1 (without damping)

| Beam | Theoretical | Estimated | Error(%) | Cable | Theoretical | Estimated | Error(%) |
|------|-------------|-----------|----------|-------|-------------|-----------|----------|
| 1    | 1.1508      | 1.1508    | 0.000    | 18    | 2.2100      | 2.2100    | 0.000    |
| 2    | 1.1508      | 1.1508    | 0.000    | 19    | 1.9900      | 1.9900    | 0.000    |
| 3    | 1.1508      | 1.1508    | 0.000    | 20    | 2.0000      | 2.0000    | 0.000    |
| 4    | 1.1508      | 1.1508    | 0.000    | 21    | 1.7600      | 1.7600    | 0.000    |
| 5    | 1.1508      | 1.1508    | 0.000    | 22    | 2.4200      | 2.4200    | 0.000    |
| 6    | 1.1508      | 1.1508    | 0.000    | 23    | 2.4500      | 2.4500    | 0.000    |
| 7    | 1.1508      | 1.1508    | 0.000    | 24    | 2.5000      | 2.5000    | 0.000    |
| 8    | 1.1508      | 1.1508    | 0.000    | 25    | 2.5400      | 2.5400    | 0.000    |
| 9    | 1.1508      | 1.1508    | 0.000    | 26    | 2.6500      | 2.6500    | 0.000    |
| 10   | 1.1508      | 1.1508    | 0.000    | 27    | 2.6300      | 2.6300    | 0.000    |
| 11   | 1.1508      | 1.1508    | 0.000    | 28    | 2.6900      | 2.6900    | 0.000    |
| 12   | 1.1508      | 1.1508    | 0.000    | 29    | 2.6000      | 2.6000    | 0.000    |
| 13   | 1.1508      | 1.1508    | 0.000    | 30    | 2.6100      | 2.6100    | 0.000    |
| 14   | 1.1508      | 1.1508    | 0.000    | 31    | 2.3700      | 2.3700    | 0.000    |
| 15   | 1.1508      | 1.1508    | 0.000    | 32    | 2.4000      | 2.4000    | 0.000    |
| 16   | 1.1508      | 1.1508    | 0.000    | 33    | 4.0200      | 4.0200    | 0.000    |
| 17   | 1.1508      | 1.1508    | 0.000    |       |             |           |          |

The time tracking of the identification processes of NO.1 beam element and NO.128 cable element are shown in Figs. 6 (a) and 6(b) respectively for illustration.

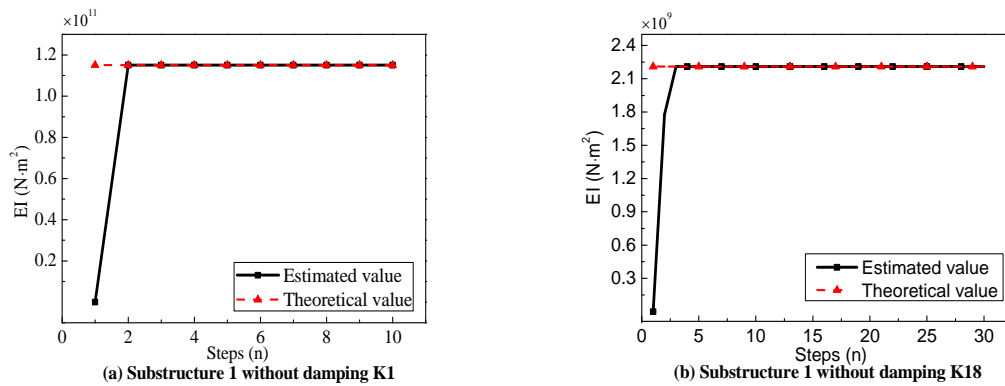


Fig. 6 The time tracking of the identification processes of substructure 1 (without damping)

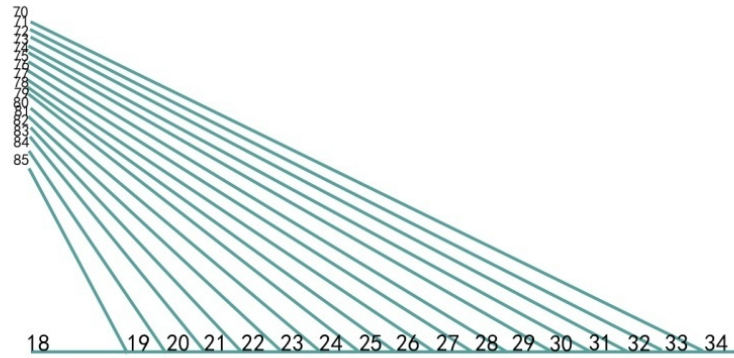


Fig. 7 Substructure 2

### Substructure 2

The beam of the right span of the bridge model and the cables attached to it are considered as substructure 2 as shown in Fig. 7.

Substructure 2 contains NO.18-34 beam elements and NO.144-159 cable elements. Similar to substructure 1, the responses at the beam nodes and the cable nodes on the tower are considered as interface DOFs. Again, there are 33 stiffness parameters to identify and the corresponding displacement vectors, parametric vectors, measurement vectors and observation matrices used in the LSE method are as follows

$$\mathbf{x} = (x_{34} \quad x_{35} \quad \cdots \quad x_{68} \quad , \quad x_{135} \quad x_{136} \quad \cdots \quad x_{165})^T \quad (37)$$

$$\boldsymbol{\theta} = (\theta_{18} \quad \theta_{19} \quad \cdots \quad \theta_{34}, \quad \theta_{144} \quad \theta_{145} \quad \cdots \quad \theta_{159})^T \quad (38)$$

$$\mathbf{y} = (y_{35} \quad y_{36} \quad \cdots \quad y_{66})^T \quad (39)$$

$$\boldsymbol{\varphi} = (\mathbf{S}_{18}^e \mathbf{x} \quad \mathbf{S}_{19}^e \mathbf{x} \quad \cdots \quad \mathbf{S}_{34}^e \mathbf{x}, \quad \mathbf{S}_{144}^e \mathbf{x} \quad \mathbf{S}_{145}^e \mathbf{x} \quad \cdots \quad \mathbf{S}_{159}^e \mathbf{x}) \quad (40)$$

The results of identified structural parameters of substructure 2 are shown in Table 3, where the numbering and units of parameters are the same as those in Table 2.

For illustration, the time tracking of the identification processes of NO.18 beam element and NO.144 cable element are shown in Figs. 8 (a) and 8(b) respectively.

### Substructure 3

The tower and all the cables attached to it are extracted as substructure 3 shown in Fig. 9.

Table 3 Identification parameters of substructure 2 (without damping)

| Beam | Theoretical | Estimated | Error(%) | Cable | Theoretical | Estimated | Error(%) |
|------|-------------|-----------|----------|-------|-------------|-----------|----------|
| 1    | 1.1508      | 1.1508    | 0.000    | 18    | 2.6000      | 2.2100    | 0.000    |
| 2    | 1.1508      | 1.1508    | 0.000    | 19    | 1.9700      | 1.9900    | 0.000    |
| 3    | 1.1508      | 1.1508    | 0.000    | 20    | 1.7200      | 2.0000    | 0.000    |
| 4    | 1.1508      | 1.1508    | 0.000    | 21    | 1.5600      | 1.7600    | 0.000    |
| 5    | 1.1508      | 1.1508    | 0.000    | 22    | 1.4000      | 2.4200    | 0.000    |
| 6    | 1.1508      | 1.1508    | 0.000    | 23    | 1.6100      | 2.4500    | 0.000    |
| 7    | 1.1508      | 1.1508    | 0.000    | 24    | 1.8000      | 2.5000    | 0.000    |
| 8    | 1.1508      | 1.1508    | 0.000    | 25    | 1.7000      | 2.5400    | 0.000    |
| 9    | 1.1508      | 1.1508    | 0.000    | 26    | 1.6700      | 2.6500    | 0.000    |
| 10   | 1.1508      | 1.1508    | 0.000    | 27    | 1.3900      | 2.6300    | 0.000    |
| 11   | 1.1508      | 1.1508    | 0.000    | 28    | 1.1900      | 2.6900    | 0.000    |
| 12   | 1.1508      | 1.1508    | 0.000    | 29    | 1.1300      | 2.6000    | 0.000    |
| 13   | 1.1508      | 1.1508    | 0.000    | 30    | 1.6300      | 2.6100    | 0.000    |
| 14   | 1.1508      | 1.1508    | 0.000    | 31    | 1.5000      | 2.3700    | 0.000    |
| 15   | 1.1508      | 1.1508    | 0.000    | 32    | 1.1900      | 2.4000    | 0.000    |
| 16   | 1.1508      | 1.1508    | 0.000    | 33    | 1.0200      | 4.0200    | 0.000    |
| 17   | 1.1508      | 1.1508    | 0.000    |       |             |           |          |

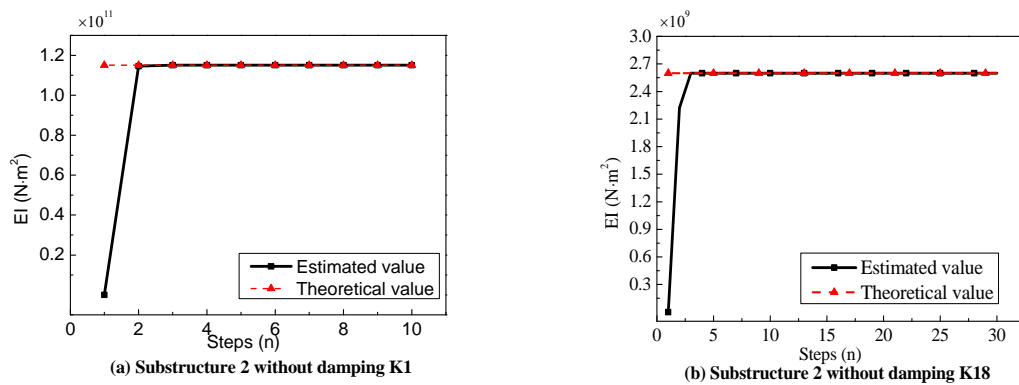


Fig. 8 The time tracking of the identification processes of substructure 2 (without damping)

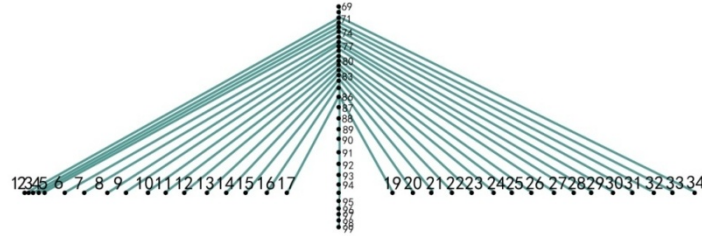


Fig. 9 Substructure 3

Substructure 3 contains NO.68-97 tower elements and NO.128-159 cable elements. The cable elements  $EA$  can be regarded as known quantities since they have already been obtained in substructure1 and 2. Therefore, in this substructure, there are only 30 stiffness parameters to be identified and the corresponding displacement vectors, parametric vectors, measurement vectors and observation matrices used in the LSE method are as follows

$$\mathbf{x} = (x_1 \quad \cdots \quad x_{33}, \quad x_{35} \quad \cdots \quad x_{66}, \quad x_{133} \quad \cdots \quad x_{192})^T \tag{41}$$

$$\boldsymbol{\theta} = (\theta_{68} \quad \theta_{69} \quad \cdots \quad \theta_{97})^T \tag{42}$$

$$\mathbf{y} = (y_{133} \quad \cdots \quad y_{192})^T - (\mathbf{S}_{128}^e \mathbf{x} \quad \mathbf{S}_{129}^e \mathbf{x} \quad \cdots \quad \mathbf{S}_{159}^e \mathbf{x})(\theta_{128} \quad \theta_{129} \quad \cdots \quad \theta_{159})^T \tag{43}$$

$$\boldsymbol{\varphi} = (\mathbf{S}_{68}^e \mathbf{x} \quad \mathbf{S}_{69}^e \mathbf{x} \quad \cdots \quad \mathbf{S}_{97}^e \mathbf{x}) \tag{44}$$

where  $(\theta_{68} \quad \theta_{69} \quad \cdots \quad \theta_{97})^T$  denote the parameters of tower elements to be identified while  $(\theta_{128} \quad \theta_{129} \quad \cdots \quad \theta_{159})^T$  denote the parameters of cable elements that have already been estimated.

Table 4 presents the identified structural parameters  $EI$  ( $10^{12} N \cdot m^2$ ) of substructure 3 and Fig. 10 plots the time tracking of the identification process of NO.68 tower element.

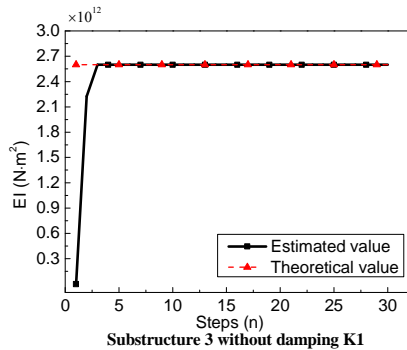


Fig. 10 The time tracking of the identification processes of substructure 3 (without damping)

Table 4 Identification parameters of substructure 3 (without damping)

| Tower | Theoretical | Estimated | Error(%) | Tower | Theoretical | Estimated | Error(%) |
|-------|-------------|-----------|----------|-------|-------------|-----------|----------|
| 1     | 3.2362      | 3.2362    | 0.000    | 16    | 3.2362      | 3.2362    | 0.000    |
| 2     | 3.2362      | 3.2362    | 0.000    | 17    | 7.7504      | 7.7504    | 0.000    |
| 3     | 3.2362      | 3.2362    | 0.000    | 18    | 7.7504      | 7.7504    | 0.000    |
| 4     | 3.2362      | 3.2362    | 0.000    | 19    | 7.7504      | 7.7504    | 0.000    |
| 5     | 3.2362      | 3.2362    | 0.000    | 20    | 7.7504      | 7.7504    | 0.000    |
| 6     | 3.2362      | 3.2362    | 0.000    | 21    | 7.7504      | 7.7504    | 0.000    |
| 7     | 3.2362      | 3.2362    | 0.000    | 22    | 7.7504      | 7.7504    | 0.000    |
| 8     | 3.2362      | 3.2362    | 0.000    | 23    | 7.7504      | 7.7504    | 0.000    |
| 9     | 3.2362      | 3.2362    | 0.000    | 24    | 7.7504      | 7.7504    | 0.000    |
| 10    | 3.2362      | 3.2362    | 0.000    | 25    | 7.7504      | 7.7504    | 0.000    |
| 11    | 3.2362      | 3.2362    | 0.000    | 26    | 7.7504      | 7.7504    | 0.000    |
| 12    | 3.2362      | 3.2362    | 0.000    | 27    | 10.981      | 10.981    | 0.000    |
| 13    | 3.2362      | 3.2362    | 0.000    | 28    | 10.981      | 10.981    | 0.000    |
| 14    | 3.2362      | 3.2362    | 0.000    | 29    | 10.981      | 10.981    | 0.000    |
| 15    | 3.2362      | 3.2362    | 0.000    | 30    | 10.981      | 10.981    | 0.000    |

#### 4.2 Structure with damping

As structural damping can only be obtained experimental, in the numerical study, Rayleigh damping will be assumed with mass damping coefficient  $\alpha = 0.001$  and stiffness damping coefficient  $\beta = 0.002$ . The parametric identification is carried out using the same substructures as in session 4.1. In addition to stiffness, the damping coefficients  $\alpha$ ,  $\beta$  will also be estimated compared to the case of structure without damping.

##### Substructure 1

There are 35 parameters to be identified in substructure 1. The corresponding displacement vectors, parametric vectors, measurement vectors and observation matrices used in the LSE method are as follows

$$\mathbf{x} = (x_1 \ x_2 \ \dots \ x_{34} \ , \ x_{135} \ x_{136} \ \dots \ x_{165})^T \tag{45}$$

$$\boldsymbol{\theta} = (\theta_1 \ \dots \ \theta_{17}, \ \theta_{128} \ \dots \ \theta_{143}, \ \beta\theta_1 \ \dots \ \beta\theta_{17}, \ \beta\theta_{128} \ \dots \ \beta\theta_{143}, \ \beta \ \alpha)^T \tag{46}$$

$$\mathbf{y} = (y_1 \quad y_2 \quad \cdots \quad y_{33})^T \quad (47)$$

$$\boldsymbol{\varphi} = (S_1^e \mathbf{x} \cdots S_{17}^e \mathbf{x}, S_{128}^e \mathbf{x} \cdots S_{143}^e \mathbf{x}, S_1^e \dot{\mathbf{x}} \cdots S_{17}^e \dot{\mathbf{x}}, S_{128}^e \dot{\mathbf{x}} \cdots S_{143}^e \dot{\mathbf{x}}, -\mathbf{K}_G \dot{\mathbf{x}} \quad \mathbf{M} \dot{\mathbf{x}}) \quad (48)$$

Table 5 presents the identified structural parameters of substructure 1 with damping, where NO.1-17 parameters represent the stiffness  $EI$  ( $10^{11} N \cdot m^2$ ) of beam elements, NO.18-33 parameters represent the stiffness  $EA$  ( $10^9 N$ ) of cable elements, NO.34-35 parameters represent the damping coefficients  $\alpha$  and  $\beta$ .

The time tracking of the identification processes of the stiffness of NO.1 beam element and NO.128 cable element as well as the damping coefficients  $\alpha$  and  $\beta$  are shown in Figs. 11 (a) - 11(d) respectively for illustration.

Table 5 Identification parameters of substructure 1 (with damping)

| Beam | Theoretical | Estimated | Error(%) | Cable | Theoretical | Estimated | Error(%) |
|------|-------------|-----------|----------|-------|-------------|-----------|----------|
| 1    | 1.151       | 1.151     | 0.000    | 18    | 2.210       | 2.210     | 0.000    |
| 2    | 1.151       | 1.151     | 0.000    | 19    | 1.990       | 1.990     | 0.000    |
| 3    | 1.151       | 1.151     | 0.000    | 20    | 2.000       | 2.000     | 0.000    |
| 4    | 1.151       | 1.151     | 0.000    | 21    | 1.760       | 1.760     | 0.000    |
| 5    | 1.151       | 1.151     | 0.000    | 22    | 2.420       | 2.420     | 0.000    |
| 6    | 1.151       | 1.151     | 0.000    | 23    | 2.450       | 2.450     | 0.000    |
| 7    | 1.151       | 1.151     | 0.000    | 24    | 2.500       | 2.500     | 0.000    |
| 8    | 1.151       | 1.151     | 0.000    | 25    | 2.540       | 2.540     | 0.000    |
| 9    | 1.151       | 1.151     | 0.000    | 26    | 2.650       | 2.650     | 0.000    |
| 10   | 1.151       | 1.151     | 0.000    | 27    | 2.630       | 2.630     | 0.000    |
| 11   | 1.151       | 1.151     | 0.000    | 28    | 2.690       | 2.690     | 0.000    |
| 12   | 1.151       | 1.151     | 0.000    | 29    | 2.600       | 2.600     | 0.000    |
| 13   | 1.151       | 1.151     | 0.000    | 30    | 2.610       | 2.610     | 0.000    |
| 14   | 1.151       | 1.151     | 0.000    | 31    | 2.370       | 2.370     | 0.000    |
| 15   | 1.151       | 1.151     | 0.000    | 32    | 2.400       | 2.400     | 0.000    |
| 16   | 1.151       | 1.151     | 0.000    | 33    | 2.210       | 2.210     | 0.000    |
| 17   | 1.151       | 1.151     | 0.000    | 34    | 0.001       | 0.001     | 0.007    |
|      |             |           |          | 35    | 0.002       | 0.002     | 0.001    |

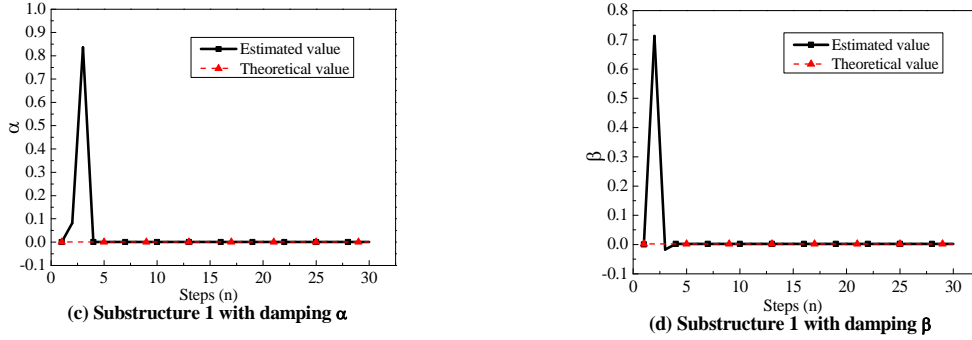


Fig. 11 The time tracking of the identification processes of substructure 1 (with damping)

### Substructure 2

There are 35 parameters to be identified. The corresponding displacement vectors, parametric vectors, measurement vectors and observation matrices used in the LSE method are as follows

$$\mathbf{x} = (x_{34} \ x_{35} \ \cdots \ x_{68} \ , \ x_{135} \ x_{136} \ \cdots \ x_{165})^T \quad (49)$$

$$\boldsymbol{\theta} = (\theta_{18} \ \cdots \ \theta_{34}, \ \theta_{144} \ \cdots \ \theta_{159}, \ \beta\theta_{18} \ \cdots \ \beta\theta_{34}, \ \beta\theta_{144} \ \cdots \ \beta\theta_{159}, \ \beta \ \alpha)^T \quad (50)$$

$$\mathbf{y} = (y_{35} \ y_{36} \ \cdots \ y_{66})^T \quad (51)$$

$$\boldsymbol{\varphi} = (\mathbf{S}_{18}^e \mathbf{x} \ \cdots \ \mathbf{S}_{34}^e \mathbf{x}, \ \mathbf{S}_{144}^e \mathbf{x} \ \cdots \ \mathbf{S}_{159}^e \mathbf{x}, \ \mathbf{S}_{18}^e \dot{\mathbf{x}} \ \cdots \ \mathbf{S}_{34}^e \dot{\mathbf{x}}, \ \mathbf{S}_{144}^e \dot{\mathbf{x}} \ \cdots \ \mathbf{S}_{159}^e \dot{\mathbf{x}}, \ -\mathbf{K}_G \dot{\mathbf{x}} \ \mathbf{M} \dot{\mathbf{x}}) \quad (52)$$

The results of identified structural parameters of substructure 2 are shown in Table 6, where the numbering and units of parameters are the same as those in Table 5.

The time tracking of the identification processes of the stiffness of NO.18 beam element and NO.144 cable element as well as the damping coefficients  $\alpha$  and  $\beta$  are shown in Figs. 12(a) - 12(d) respectively.

### Substructure 3

There are 32 parameters to be identified. The corresponding displacement vectors, parametric vectors, measurement vectors and observation matrices used in the LSE method are as follows

$$\mathbf{x} = (x_1 \ \cdots \ x_{33}, \ x_{35} \ \cdots \ x_{66}, \ x_{133} \ \cdots \ x_{192})^T \quad (53)$$

$$\boldsymbol{\theta} = (\theta_{68} \ \theta_{69} \ \cdots \ \theta_{97}, \ \beta\theta_{68} \ \beta\theta_{69} \ \cdots \ \beta\theta_{97}, \ \beta \ \alpha)^T \quad (54)$$

$$\mathbf{y} = (y_{133} \ \cdots \ y_{192})^T - (\mathbf{S}_{128}^e \mathbf{x} \ \mathbf{S}_{129}^e \mathbf{x} \ \cdots \ \mathbf{S}_{159}^e \mathbf{x}) (\theta_{128} \ \theta_{129} \ \cdots \ \theta_{159})^T - (\mathbf{S}_{128}^e \dot{\mathbf{x}} \ \mathbf{S}_{129}^e \dot{\mathbf{x}} \ \cdots \ \mathbf{S}_{159}^e \dot{\mathbf{x}}) (\beta\theta_{128} \ \beta\theta_{129} \ \cdots \ \beta\theta_{159})^T \quad (55)$$

$$\boldsymbol{\varphi} = \left( S_{68}^e \mathbf{x} \quad S_{69}^e \mathbf{x} \quad \cdots \quad S_{97}^e \mathbf{x}, \quad S_{68}^e \dot{\mathbf{x}} \quad S_{69}^e \dot{\mathbf{x}} \quad \cdots \quad S_{97}^e \dot{\mathbf{x}}, \quad -\mathbf{K}_G \dot{\mathbf{x}} \quad \mathbf{M} \dot{\mathbf{x}} \right) \quad (56)$$

where  $(\theta_{128} \quad \theta_{129} \quad \cdots \quad \theta_{159})^T$  and  $(\beta\theta_{128} \quad \beta\theta_{129} \quad \cdots \quad \beta\theta_{159})^T$  denote the cable elements parameters  $EA$  and  $\beta EA$  that have already been obtained in substructures 1 and 2.

The identification results of structural parameters of substructure 3 are summarized in Table 7, where NO.1-30 parameters represent the stiffness  $EI$  ( $10^{12} N \cdot m^2$ ) of tower elements and NO.31-32 parameters represent the damping coefficients  $\alpha$  and  $\beta$ .

The time tracking of the identification processes of the stiffness of NO.68 tower element, as well as the damping coefficients  $\alpha$  and  $\beta$  are shown in Figs. 13 (a) - 13(c) respectively.

Table 6 Identification parameters of substructure 2 (with damping)

| Beam | Theoretical | Estimated | Error(%) | Cable | Theoretical | Estimated | Error(%) |
|------|-------------|-----------|----------|-------|-------------|-----------|----------|
| 1    | 1.151       | 1.151     | 0.000    | 18    | 2.600       | 2.600     | 0.000    |
| 2    | 1.151       | 1.151     | 0.000    | 19    | 1.970       | 1.970     | 0.000    |
| 3    | 1.151       | 1.151     | 0.000    | 20    | 1.720       | 1.720     | 0.000    |
| 4    | 1.151       | 1.151     | 0.000    | 21    | 1.560       | 1.560     | 0.000    |
| 5    | 1.151       | 1.151     | 0.000    | 22    | 1.400       | 1.400     | 0.000    |
| 6    | 1.151       | 1.151     | 0.000    | 23    | 1.610       | 1.610     | 0.000    |
| 7    | 1.151       | 1.151     | 0.000    | 24    | 1.800       | 1.800     | 0.000    |
| 8    | 1.151       | 1.151     | 0.000    | 25    | 1.700       | 1.700     | 0.000    |
| 9    | 1.151       | 1.151     | 0.000    | 26    | 1.670       | 1.670     | 0.000    |
| 10   | 1.151       | 1.151     | 0.000    | 27    | 1.390       | 1.390     | 0.000    |
| 11   | 1.151       | 1.151     | 0.000    | 28    | 1.190       | 1.190     | 0.000    |
| 12   | 1.151       | 1.151     | 0.000    | 29    | 1.130       | 1.130     | 0.000    |
| 13   | 1.151       | 1.151     | 0.000    | 30    | 1.630       | 1.630     | 0.000    |
| 14   | 1.151       | 1.151     | 0.000    | 31    | 1.500       | 1.500     | 0.000    |
| 15   | 1.151       | 1.151     | 0.000    | 32    | 1.190       | 1.190     | 0.000    |
| 16   | 1.151       | 1.151     | 0.000    | 33    | 1.020       | 1.020     | 0.000    |
| 17   | 1.151       | 1.151     | 0.000    | 34    | 0.001       | 0.001     | 0.001    |
|      |             |           |          | 35    | 0.002       | 0.002     | 0.001    |

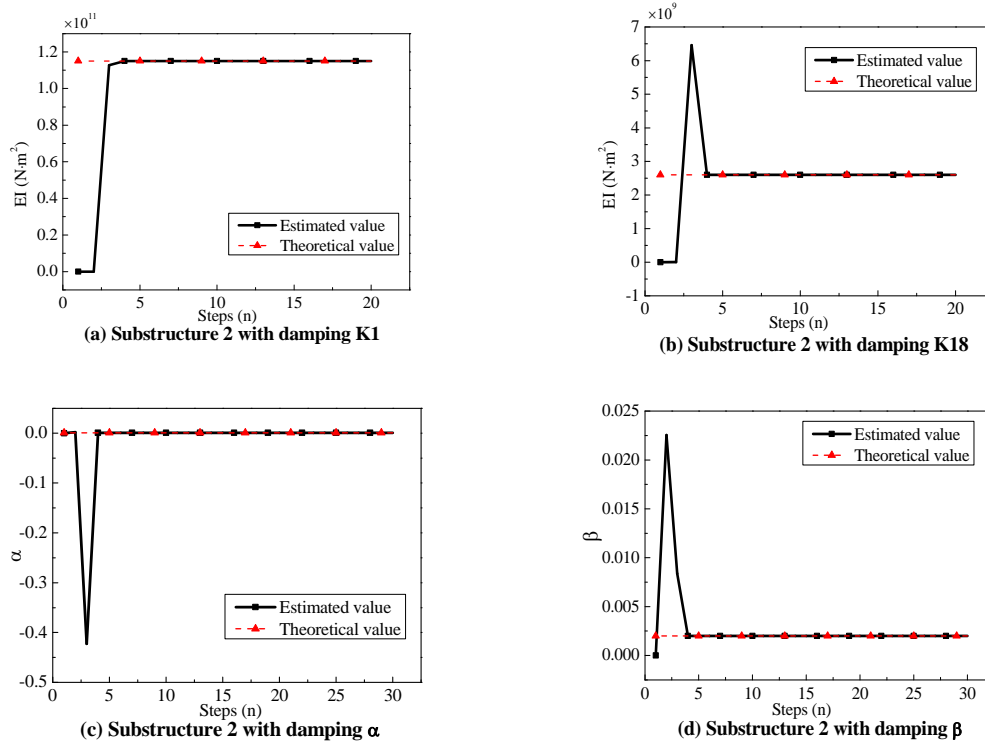


Fig. 12 The time tracking of the identification processes of substructure 2 (with damping)

Table 7 Identification results of Substructure 3 with damping

| Tower | Theoretical | Estimated | Error(%) | Tower | Theoretical | Estimated | Error(%) |
|-------|-------------|-----------|----------|-------|-------------|-----------|----------|
| 1     | 3.236       | 3.236     | 0.000    | 17    | 7.750       | 7.750     | 0.000    |
| 2     | 3.236       | 3.236     | 0.000    | 18    | 7.750       | 7.750     | 0.000    |
| 3     | 3.236       | 3.236     | 0.000    | 19    | 7.750       | 7.750     | 0.000    |
| 4     | 3.236       | 3.236     | 0.000    | 20    | 7.750       | 7.750     | 0.000    |
| 5     | 3.236       | 3.236     | 0.000    | 21    | 7.750       | 7.750     | 0.000    |
| 6     | 3.236       | 3.236     | 0.000    | 22    | 7.750       | 7.750     | 0.000    |
| 7     | 3.236       | 3.236     | 0.000    | 23    | 7.750       | 7.750     | 0.000    |
| 8     | 3.236       | 3.236     | 0.000    | 24    | 7.750       | 7.750     | 0.000    |
| 9     | 3.236       | 3.236     | 0.000    | 25    | 7.750       | 7.750     | 0.000    |
| 10    | 3.236       | 3.236     | 0.000    | 26    | 7.750       | 7.750     | 0.000    |
| 11    | 3.236       | 3.236     | 0.000    | 27    | 10.981      | 10.981    | 0.000    |
| 12    | 3.236       | 3.236     | 0.000    | 28    | 10.981      | 10.981    | 0.000    |
| 13    | 3.236       | 3.236     | 0.000    | 29    | 10.981      | 10.981    | 0.000    |
| 14    | 3.236       | 3.236     | 0.000    | 30    | 10.981      | 10.981    | 0.000    |
| 15    | 3.236       | 3.236     | 0.000    | 31    | 0.001       | 9.99e-4   | -0.006   |
| 16    | 3.236       | 3.236     | 0.000    | 32    | 0.002       | 0.002     | 0.000    |

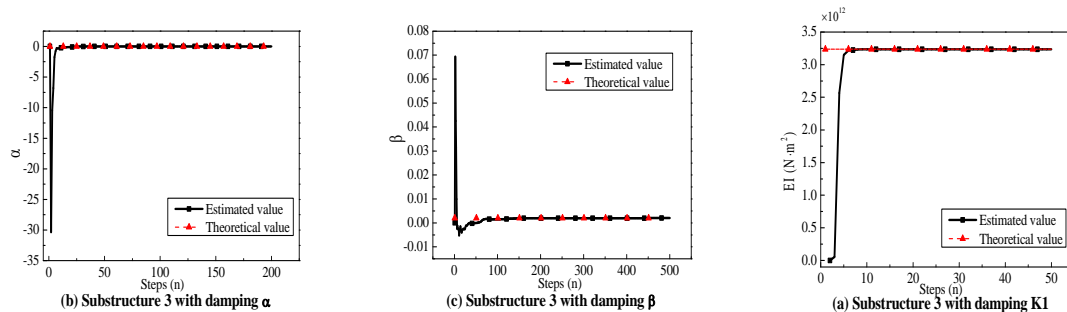


Fig. 13 The time tracking of identification processes of substructure 3 (with damping)

### 4.3 Summary

It can be seen from the simulation results given in Tables 2-7 that using the proposed LSE method combined with substructure approach, the parameters of all the elements of the entire bridge model can be computed progressively from substructure to substructure. Also, the identified structural parameters can be tracked real-time or online as shown in Figs. 6, 8 and 10-13. Finally, it proves that without measurement noises, the proposed method can estimate structural parameters with very high accuracy, no matter whether the structure is without or with damping.

## 5. Conclusions

In this paper, the LSE method has been used combined with a substructure approach for the identification of structural parameters of a cable-stay bridge with large DOFs. Numerical analysis has been carried out based on the simplified 2D model of the bridge under vertical white noise excitations. Three substructures are extracted from the full finite element model of the bridge and the parameters of each substructure are estimated. The simulation results show that the proposed identification method has a high accuracy without measurement noises, and it is especially suitable for large structures with repeated patterns where the substructure approach can reduce the complexity of the problem and the LSE method can efficiently compute the structural parameters. However, the classic LSE method requires full measurements at every DOF which is usually not possible in real practice. Therefore, further studies have to be carried out to extend the LSE method to cover the case of incomplete measurement, and also the effect of different external excitations and measurement noises have to be investigated.

## Acknowledgments

This research is partially supported by the Science and Technology Commission of Shanghai Municipality (Grant Nos. 13ZR1443400) and the National Basic Research Program of China (973 Program) (Grant Nos. 2013CB036300).

## References

- Bernal, D., and Beck, J. (2004), "Special section: Phase I of the IASC-ASCE structural health monitoring benchmark", *J. Eng. Mech. - ASCE*, **130**(1), 1-127.
- Caravani, P., Watson, M.L. and Thomson, W.T. (1977), "Recursive least-squares time domain identification of structural parameters", *J. Appl. Mech. - T ASME*, **44**(1), 135-140.
- Dong, S. and Sun, L.M. (2010), *Extreme load identification and early warning research of cable-stayed bridge based on monitoring data*, Master Thesis, Tongji University, Shanghai, China.
- Koh, C.G., Hong, B. and Liaw, C.Y. (2003), "Substructural and progressive structural identification methods", *Eng. Struct.*, **25**(12), 1551-1563.
- Koh, C.G., See, L.M. and Balendra, T. (1991), "Estimation of structural parameters in time domain: a substructure approach", *Earthq. Eng. Struct. D.*, **20**(8), 787-801.
- Law, S.S. and Yong, D. (2011), "Substructure methods for structural condition assessment", *J. Sound Vib.*, **330**(15), 3606-3619.
- Lei, Y, Jiang, Y.Q. and Xu, Z.Q. (2012), "Structural damage detection With limited input and output measurement signals", *Mech. Syst. Signal Pr.*, **28**, 229-243.
- Lei, Y., Liu, C., Jiang, Y.Q. and Mao, Y.K. (2013), "Substructure based structural damage detection with limited input and output measurements", *Smart Struct. Syst.*, **12**(6), 619-640.
- Lin, S., Yang, J.N. and Zhou, L. (2005), "Damage identification of a benchmark problem for structural health monitoring", *J. Smart Mater. Struct.*, **14**, S162-S169.
- Weng, S., Xia, Y. and Zhou, X.Q. (2012), "Inverse substructure method for model updating of structures", *J. Sound Vib.*, **331**(25), 5449-5468.
- Yang, J.N. and Lin, S. (2004), "On-line identification of nonlinear hysteretic structures using an adaptive tracking technique", *Int. J. Nonlinear Mech.*, **39**, 1481-1491.
- Yang, J.N. and Lin, S. (2005), "Identification of parametric variations of structures based on least squares estimation and adaptive tracking technique", *J. Eng. Mech. - ASCE*, **131**(3), 290-298.
- Yang, J.N., Pan, S. and Lin, S. (2007a), "Least squares estimation with unknown excitations for damage identification of structures", *J. Eng. Mech. - ASCE*, **133**(1), 12-21.
- Yi, T.H., Li, H.N. and Gu, M. (2010), "Full-scale measurement of dynamic response of a suspension bridge subjected to environmental loads using GPS technology", *Science China: Technol. Sci.*, **53**(2), 469-479.
- Yi, T.H., Li, H.N. and Gu, M. (2013a), "Wavelet based multi-step filtering method for bridge health monitoring using GPS and accelerometer", *Smart Struct. Syst.*, **11**(4), 331-348.
- Yi, T.H., Li, H.N. and Sun, H.M. (2013b), "Multi-stage structural damage diagnosis method based on "Energy-Damage" theory", *Smart Struct. Syst.*, **12**(3-4), 345-361.
- Zhou, L. and Yan, G. (2006), "HHT method for system identification and damage detection: an experimental study", *Smart Struct. Syst.*, **2**(2), 141-154.